minerals

MDPI

Article

In Situ Hydrophobization of Lithium Aluminate Particles for Flotations by Dry Grinding in the Presence of Punicines

Frédéric Steiner [1], Ali Zgheib [2], Maximilian Hans Fischer [2], Lukas Büttner [1], Andreas Schmidt [2,*] and Sandra Breitung-Faes [1,*]

[1] Technische Hochschule Nürnberg Georg Simon Ohm, Faculty of Process Engineering, Mechanical Process Engineering/Particle Technology, Wassertorstraße 10, 90403 Nuremberg, Germany; steinerfr68668@th-nuernberg.de (F.S.); lukas.buettner@th-nuernberg.de (L.B.)

[2] Institute of Organic Chemistry, Clausthal University of Technology, Leibnizstraße 6, 38678 Clausthal-Zellerfeld, Germany; ali.zgheib@tu-clausthal.de (A.Z.); mf39@tu-clausthal.de (M.H.F.)

* Correspondence: schmidt@ioc.tu-clausthal.de (A.S.); sandra.breitung-faes@th-nuernberg.de (S.B.-F.); Tel.: +49-5323-72-3861 (A.S.); +49-911-5880-1605 (S.B.-F.)

Abstract: The engineered artificial mineral (EnAM) lithium aluminate ($LiAlO_2$) is a promising candidate for the recycling of lithium from slags, which can originate from the reprocessing of batteries, for example. Derivatives of the natural product Punicine (1-(2′,5′-dihydroxyphenyl)-pyridinium) from *Punica granatum* have been proven to be effective switchable collectors for the flotation of this mineral as they react to light. In the present study, three Punicines were added to a planetary ball mill before grinding $LiAlO_2$ to particle sizes suitable for flotation. We investigated the influence of Punicine and two derivatives with C10 and C17 side chains on the grinding results at different grinding times and conditions as well as on the yields in flotations. SEM images of the particles, IR and ICP–OES measurements provided insights into the Punicine–particle interactions. They showed that Punicines not only prevent the formation of hydrophilic and thus undesirable lithium aluminate hydroxide hydrate ($LiAl_2(OH)_7 \blacksquare x\ H_2O$) surfaces in this process, as is unavoidable in aqueous flotation without this pretreatment, they also prevent the undesired release of lithium cations into the aqueous phase. Due to considerable hydrophobization of the particle surface of $LiAlO_2$, nearly quantitative recovery rates of this engineered artificial mineral are achieved using the process described here.

Keywords: lithium; recycling; planetary ball mill; comminution; engineered artificial mineral; EnAM; collector; flotation; recovery

Citation: Steiner, F.; Zgheib, A.; Fischer, M.H.; Büttner, L.; Schmidt, A.; Breitung-Faes, S. In Situ Hydrophobization of Lithium Aluminate Particles for Flotations by Dry Grinding in the Presence of Punicines. *Minerals* **2024**, *14*, 650. https://doi.org/10.3390/min14070650

Academic Editor: Kevin Galvin

Received: 16 May 2024
Revised: 20 June 2024
Accepted: 21 June 2024
Published: 25 June 2024

1. Introduction

In order to achieve the climate targets and the planned progress in the area of digitalization, considerable efforts are required in Europe in the extraction, processing and recovery of critical raw materials. For this reason, the European Raw Materials Act was passed [1], in which special importance was attached to lithium, among other elements. The demand for lithium carbonate equivalents will be over 2.4 million tons in 2030 and is expected to be twice as high as in 2025 [2]. In addition to battery production, particularly for the development of e-mobility, lithium is also used in the ceramics industry [3–5], glass production [6,7], lubricants [8,9] and coolants [10,11] as well as in the nuclear industry [12] and optoelectronics [13]. Today, pyrometallurgical treatment is an important process for the recycling of lithium-ion batteries. The elements copper, cobalt and nickel form alloys, while lithium is mainly contained in the slag [14,15], which has suddenly become the focus of interest. Processing technology projects are currently intensively investigating which processes can be used to specifically produce lithium-rich artificial minerals in the slag, how these can be effectively separated and finally how lithium-rich concentrates that are suitable for subsequent hydrometallurgical processing can be produced. Lithium

aluminate ($LiAlO_2$) is a so-called engineered artificial mineral (EnAM) that forms from mixtures consisting of lithium oxide, aluminum oxide, silicon dioxide and calcium oxide. Its formation can be triggered by the addition of aluminum during the pyrometallurgical process. The influence of other compounds, including those containing manganese or magnesium, is also currently being carefully investigated [16]. Once the desired engineered artificial minerals such as $LiAlO_2$ have been formed, another challenge is the mechanical separation of the target minerals from gangue materials, which often form interlocking particles with them, by crushing and grinding the slag. Ideally, this results in particles that are available for further processing, e.g., a flotation step for separating the gangue material from the valuable components.

The comminution steps can be divided into coarse and fine comminution as well as wet and dry processes, depending on the size of the input particles and the comminution environment. Chelgani et al. make a comparison between dry and wet grinding as preparation of ores for flotation [17]. Dry comminution is less efficient in terms of energy efficiency but is gaining interest as water is a rare constituent in some regions of the world. Wet comminution can produce finer particles, while dry comminution can lead to the agglomeration of powders with increasing fineness, resulting in caking, transportation and handling problems. However, dry comminution is reported to be more reactive and allows for amorphization, phase transformations or chemical reactions [18,19]. Another factor to consider when choosing the comminution method is the interaction between liquids and solids. The creation of new surfaces can lead to increased solubility effects in wet processes, which can be counterproductive for flotation [20,21]. This aspect occurs when grinding lithium aluminate in an aqueous phase. In addition, wear is lower with dry comminution, which is advantageous for many types of raw materials [22–24]. There are numerous publications on the interactions between comminution conditions using the example of copper or sulphate raw materials [25–28]. With regard to the element lithium, Zhu et al. investigated the flotation of the Li-bearing mineral spodumene and found that the selectivity of binding flotation additives was impaired by dry comminution [29]. Xu et al. investigated the influence of particle size on spodumene flotation and showed that decreasing particle size has a slightly negative effect, while pH has a significantly stronger influence on yield [30]. This result was confirmed by Zhu et al. [31]. Thanua et al. added collector additives during the comminution of spodumene and observed a significant increase in yield during dry comminution with additives, although the selectivity decreased [32]. This was attributed to the chemical activation of silicate phases, such as aluminates, during dry processing. Thus, a dry process will be used here for the lithium aluminate, as the reactivity of the newly built surface should be used while avoiding any solubility effects of lithium already during grinding.

Flotation, which is based on the different surface hydrophobicity of the dispersed particles, is a very effective method for separating particles of the desired minerals from gangue materials [33–36]. After the formation of an aqueous suspension and conditioning with a selection of suitable reagents such as collectors, foaming agents, depressants, activators and regulators, the air is introduced into the dispersion, causing the hydrophobized particles to collide with and attach to the rising air bubbles. The hydrophilic particles, on the other hand, remain suspended in the pulp. The reagents mentioned thus influence the interfacial properties of particles and air bubbles, which, in addition to the hydrodynamic parameters, are decisive for the success of the flotation [37]. In view of the new challenges in the field of recycling, new flotation conditions are being intensively investigated. The aim is to maximize the adsorption of the particles on the surfaces in order to selectively increase the hydrophobicity of the particles and thus improve the attractive interactions between particles and air bubbles [38–41] and optimize selectivity. Sodium oleate is often used as a surface-active collector for the flotation of lithium-bearing minerals [42], but other collectors have also been investigated [43].

From the fact that aqueous suspensions of lithium aluminate have a pH value of 11, it can be concluded that the mineral is not completely insoluble in water, contrary to

what is stated in the literature [44] and that hydroxide ions are formed through a reaction with water [45]. This conversion can be described by the reaction equations listed below; they lead to lithium hydroxide and lithium aluminum hydroxide hydrate $LiAl_2(OH)_7 \blacksquare x\ H_2O$ on the surface [46–49]. On the one hand, this reaction with water is unfavorable for flotation because it hydrophilizes the particle surfaces. On the other hand, it enables the development of collectors that can exchange the hydroxide groups of the lithium aluminum hydroxide hydrate by nucleophilic substitution and thus form chemical bonds with the surface. In fact, the *Schmidt* group was able to carry out very effective flotations using Punicines as novel switchable collectors [45,50] as explained in more detail below. Carbon dioxide from the air eventually leads to the formation of carbonates.

$$2\ LiAlO_2 + (4 + x)\ H_2O \rightarrow LiAl_2(OH)_7 \blacksquare x\ H_2O + LiOH \quad (1)$$

$$LiAl_2(OH)_7 \blacksquare 2\ H_2O + OH^- \rightarrow Li^+ + 2\ Al(OH)_4^- + 2\ H_2O \quad (2)$$

Punicine was isolated from the leaves of the pomegranate tree (*Punica granatum*) and is thus a natural product in its unsubstituted form (Scheme 1) [51]. It was later investigated in more detail with regard to its properties by the *Schmidt* group, especially its structure as a function of pH [52]. It is easily, cost-effectively and abundantly accessible through simple syntheses [53–55]. Punicine combines an electron-poor (pyridinium) and an electron-rich aromatic compound (hydroquinone) in its cationic, i.e., completely protonated, form. This stabilizes olates, such as those formed by deprotonation of one of the two hydroxide groups in the hydroquinone moiety, by the adjacent cation [52]. For the above-mentioned application in the surface modification of undesirably hydrated lithium aluminate, the nucleophilic power of a stabilized olate can therefore be used for the reaction. In fact, Punicine is present as a cation in the acidic state and as a tautomeric equilibrium of two mesomeric betaines **A** and **B** in the neutral state [52]. By further increasing the pH value, Punicine changes into a tripolar anionic molecule in order to undergo ring opening to a dianion by further addition of hydroxide ions. All these steps are reversible. The special feature of Punicine, however, is its ability to form radicals when exposed to light. Scheme 1 shows one of several mesomeric structures of the possible radical cations and radical anions that were the basis for the development of photoresponsive materials [56,57] and systems for photoinduced electron transfer [58]. All states of the natural product Punicine and its derivatives have different physical properties and intermolecular interactions [59].

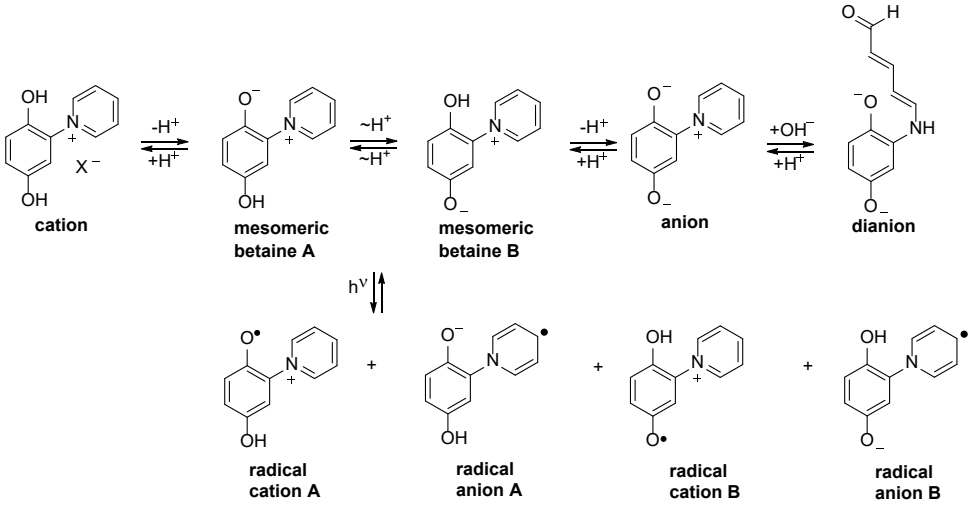

Scheme 1. The natural product Punicine can exist in different states depending on pH and light.

These properties of Punicines can be utilized to develop switchable collectors and the first results of selective flotations of lithium aluminate, galaxite and spodumene under suppression of the gangue material gehlenite are already available [45,50]. Thus, flotations

in daylight provide different results to those in the dark or when irradiated with UV light. The same applies when the pH value is changed. In addition to photoswitchability, it is primarily the nucleophilic olate functions that have been shown to react with the particle surfaces of lithium aluminate hydroxide hydrates, to which, at least in part, the hydrophobization essential for flotation can be attributed (Scheme 2).

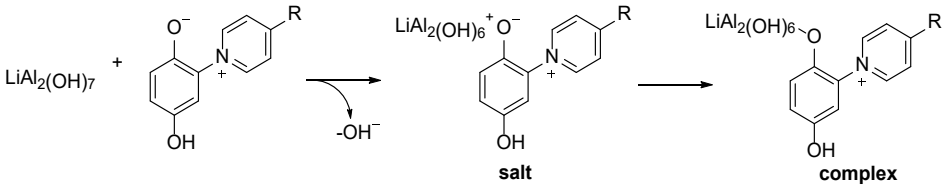

Scheme 2. Nucleophilic substitution of Punicines with the hydrated lithium aluminate surface under aqueous conditions.

Data on the toxicity of Punicine are not yet available. However, its partial structure hydroquinone is found in many plant-based foods such as wheat, pears, coffee, onions, tea and red wine and is absorbed by the gastrointestinal tract. It is described as toxic to aquatic organisms and has low toxicity to fungi and bacteria and, despite its occurrence, is considered a haematotoxic and carcinogenic agent [60,61]. Pyridine, the second partial structure of Punicine, is readily degraded in soil [62].

In continuation of this project on the recycling of lithium as an engineered artificial mineral, the aim of the present study was to hydrophobize the lithium aluminate particles in situ, i.e., during comminution and grinding by Punicines, before a reaction between the lithium aluminate and water can take place under the aqueous conditions of flotation. This should suppress the formation of lithium aluminate hydroxide hydrates and thus the loss of lithium ions into the aqueous phase. We were encouraged by the fact that water only has a nucleophilicity index N_+ of 5.16 (measured as H_2O:MeCN = 91:9) [63] while phenolates such as 4-methoxyphenolate as a model for the Punicines, whose nucleophilicity indices are not yet known, are far better nucleophiles with an index of 20.62 (in MeCN) [64]. All in all, it is to a certain extent a comparison of the dry and aqueous effects of Punicines on lithium aluminate for the benefit of flotation.

2. Materials and Methods

2.1. General

All chemicals for this project were purchased from commercial suppliers and used without further purification. ^{1}H and ^{13}C NMR spectra were measured on the BRUKER Avance (400 MHz) and an Avance III (600 MHz) NMR spectrometer (Billerica, MA, USA) at the Clausthal University of Technology. The multiplicities are indicated below with the following abbreviations: s = singlet, bs = broad singlet, d = doublet, dd = doublet of a doublet, t = triplet, tt = triplet of a triplet, q = quartet, quint = quintet, m = multiplet. For the ^{13}C/DEPT-spectra, (+) is added for carbons bonded to one or three hydrogen atoms and (−) for carbon atoms bonded to two hydrogens. Quaternary carbon atoms are denoted with the symbol (o). An Alpha-T FT-IR spectrometer from BRUKER with a platinum ATR module was used to produce the IR spectra. The spectra cover a range from 400 to 4000 cm^{-1}. The high-resolution mass spectra were measured with an Impact II mass spectrometer from BRUKER. The unsubstituted Punicine was prepared as previously described [52].

2.2. Syntheses

Three Punicine derivatives were investigated as additives in the lithium aluminate comminution process and their effects on the froth flotation process. In order to modulate the hydrophobizing effect, these additives contained different alkyl chain lengths in the 4-position of the pyridinium moiety. The target Punicines were synthesized by reacting 1,4-benzoquinone with the corresponding functionalized pyridine compounds according to the methods described in the literature. Precipitation of the chloride salt with hydrochloric

acid gave good to excellent yields of the target molecules [52]. The corresponding pyridines as starting material were synthesized by deprotonation of 4-methylpyridine via lithium diisopropylamine and subsequent alkylation (Scheme 3).

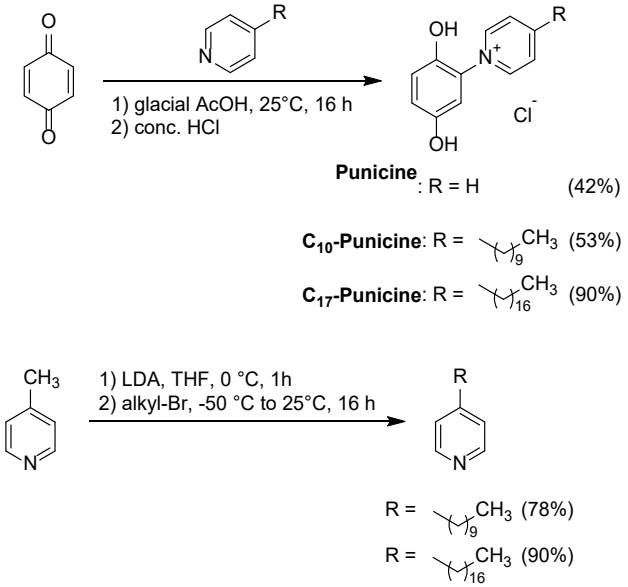

Scheme 3. Synthesis of the Punicine derivatives (not alkylated, R = H, the natural product Punicine from *Punica granatum*), C_{10}-Punicine possessing a decyl-chain, and C_{17}-Punicine possessing a heptadecyl-chain.

2.2.1. Synthesis of 1-(2′,5′-Dihydroxyphenyl)-4-Decanylpyridinium Chloride, C_{10}-Punicine

A 0.490 g sample of *p*-benzoquinone (4.56 mmol) was suspended in 10 mL of glacial acetic acid. Then, 1.000 g of 4-heptadecanylpyridine (4.56 mmol) was added. The reaction mixture was stirred at room temperature overnight. After completion, 1 mL of conc. aqueous HCl and 10 mL of pure water were added, whereupon the product precipitated and was filtered off. Yield: 0.88 g (53%), yellow solid.

2.2.2. Synthesis of 1-(2′,5′-Dihydroxyphenyl)-4-Heptadecanylpyridinium Chloride, C_{17}-Punicine)

A 2.671 g sample of *p*-benzoquinone (24.7 mmol) was suspended in 40 mL of glacial acetic acid. Then, 7.846 g of 4-heptadecanylpyridine (27.7 mmol) was added. The reaction mixture was stirred at room temperature overnight. After completion, 4 mL of conc. HCl and 20 mL of pure water were added, whereupon the product precipitated and was filtered off. Yield: 10.238 g (90%), yellow solid.

2.3. Comminution

Comminution was conducted using the planetary ball mill PULVERISETTE 7 premium line (FRITSCH GmbH, Idar-Oberstein, Germany). Two 8o ml zirconium oxide-coated grinding chambers were employed, each filled with 250 zirconium oxide grinding balls measuring 5 mm in diameter, branded as SiliBeads type ZY 6.0 (SIGMUND LINDNER GmbH, Warmensteinach, Germany) resulting in a grinding media filling ratio φ_{GM} of 0.36. Various grinding parameters, including the rotational speed of the sun disk and grinding time, were adjusted to achieve three sets of conditions: 400 rpm for 3 min, 400 rpm for 6 min and 600 rpm for 6 min. The feed material comprised 15 g of lithium aluminate (THERMO FISHER SCIENTIFIC, Waltham, Massachusetts, Us, CAS: 12003-67-7). The material was ground either in its pure form or with the addition of one of the Punicine additives (natural C_0-, C_{10}- and C_{17}-Punicine), each of which was varied by weight, i.e., 0.5%, 1% and 5% of the lithium aluminate mass. Ground material samples were vacuum-sealed in plastic

bags and shielded from light for subsequent froth flotation experiments or stored in plastic containers for further particle size and specific surface area analysis.

2.4. Froth Flotation

To evaluate the effect of Punicines as hydrophobizing agents in the mineral comminution process, microflotation experiments were conducted in 250 mL HALLIMOND tubes made of Pyrex glass. They possess a medium-pore-fritted glass through which air is dispersed into the apparatus. The airflow was adjusted to 32 cm^3/min. A magnet stirrer with a continuous stirring speed of 500 rpm kept the dispersion thoroughly mixed. In each experiment, 1.00 g of previously prepared $LiAlO_2$ was subject to flotation, and samples varied in terms of the added Punicine as well as grinding parameters. As a frother, 30 µL of 1% pine oil emulsion in water was added. As no further pH adjustments were performed, flotation took place at pH = 11, which is the natural pH of lithium aluminate dispersion in water. The samples were left to condition for 2 min (1 min in the mineral and 25 mL water; 1 min after adding frother). After conditioning, the HALLIMOND tube was filled with pure water to reach 250 mL and flotation was carried out for three minutes. The floated mineral fraction (concentrate) was then separated via the funnel trap. Tailings remained in the fritted tube and were collected. Concentrate and tailings were then filtered off and dried for 24 h at 80 °C. Recovery yields were calculated from the mass ratios of concentrate and the residing tailings. Experiments were repeated at least three times, and the confidence interval (95%) was calculated. Light scenarios of flotation were also varied, as previous research has confirmed an effect of the light scenario on the recovery rates of $LiAlO_2$ using Punicine solutions as collectors for froth flotation [50]. We varied between daylight flotation (>5000 lux) and irradiation with UV light (390–400 nm, 4500 lux). The UV experiments were conducted in a closed box (60 × 60 × 60 cm) in which the HALLIMOND tube was installed. From each wall, four LEDs from AVONEC (Wesel, Germany) (Premium 3W LED, 390–400 nm, color: UV-A, max. power: 750 mA, operating voltage: 3.5 V–4.5 V) operated via a power supply unit (APC-16-700, input: 100–240 V, output: +24 V, max. 700 mA, class 2 power supply) irradiated the tube. The wavelength 390–400 nm was chosen since Punicines at pH 11 possess an absorption maximum at this wavelength range (c.f. Supplementary Materials for UV-Vis spectra).

2.5. Analytics

2.5.1. Laser Diffraction

To characterize the comminution outcome, the particle size distribution was determined using laser diffraction analysis. This analysis was carried out using a HELOS KR (SYMPATEC GmbH, Clausthal-Zellerfeld, Germany) particle size analyzer equipped with R1, R3 and R5 lenses, enabling measurement within the range of 0.18–875 µm. The wet dispersion unit QUIXEL (SYMPATEC GmbH) was utilized with de-ionized water as the dispersion medium. Samples that posed dispersion challenges were subjected to 60 s of ultrasonication and treated with the wetting agent Tween 80 (CARL ROTH GmbH, Karlsruhe, Germany, polysorbate 80). Samples were introduced into the dispersion unit until a sufficient optical concentration was attained.

2.5.2. BET Adsorption

Further characterization of the comminution results was carried out by measuring the specific surface area of the samples using BET (Brunauer–Emmet–Teller) adsorption. This measurement was conducted on a NOVA 2000e Surface Area and Pore Size Analyzer (QUANTACHROME INSTRUMENTS, Odelzhausen, Germany) employing nitrogen gas as the adsorbate. After the removal of water at 50 °C under vacuum conditions, measurements were performed at a temperature of −196 °C using liquid nitrogen.

2.5.3. ICP–OES

Inductive Coupled Plasma–Optical Electron Spectroscopy measurements were performed on the VARIAN ICP–OES Vista MPX (now AGILENT, Santa Clara, CA, USA) and assessed with the VARIAN ICP-Expert 7.6.2 software. Samples were subjected to a second filtration prior to measurement.

2.5.4. SEM Imaging

SEM images were taken on the ZEISS Gemini DSM 982 (Oberkochen, Germany). Samples were sputtered with gold to introduce conductivity. Resolution and voltage are given with their respective images.

3. Results and Discussion

3.1. Effect of Punicine Additives on the Comminution Process and Grinding Results

The comminution of lithium aluminates with and without Punicines was carried out in the planetary ball mill for various comminution times and speeds. Since planetary ball mills do not typically have power consumption measurements, the stress model by Kwade et al. [65,66], which was adapted by Burmeister et al. for dry comminution in planetary ball mills to determine an energy-equivalent value $E_{m,eq}$ for varying operating parameters [67], was used. The specific energy represents, in combination with the particle size or the specific surface, the so-called signature plots for grinding experiments. These are used to compare the influence of parameter variations as well as for scaling and mill transfer reasons.

This calculation is based on the assumption that the stress energy $\overline{SE}$ is proportional to the kinetic energy of the grinding media transferred per collision, and when summed over the collision frequency CF, it results in a term proportional to the power consumption of a planetary ball mill jar P_{eq}. According to Burmeister et al., the stress energy for dry comminution in planetary ball mills is calculated according to Equation (3), with the sun wheel rotational speed n_{sun}, the grinding media diameter d_{GM} and the grinding media filling ratio φ_{GM}:

$$\overline{SE} = c1 \cdot n_{sun}^{2.67} \cdot d_{GM}^{3.85} \cdot \varphi_{GM}^{0.5} \quad (3)$$

where the constant $c1$ takes into account factors such as friction and damping behavior resulting from the product. The collision frequency CF can also be estimated according to Burmeister et al., and essentially contains the same parameters as the stress energy.

$$CF = c2 \cdot n_{sun}^{0.42} \cdot d_{GM}^{-3.93} \cdot \varphi_{GM}^{1.18} \quad (4)$$

The power input is simplified as the sum of the stress energy and collision frequency. The constants $c1$ and $c2$ are unknown in this case and are therefore neglected. It follows:

$$P_{eq} \sim CF \cdot \overline{SE} \quad (5)$$

Accordingly, by multiplying with the comminution time t and dividing by the product mass (mass of lithium aluminate $m_{Li-Aluminate}$ and mass of Punicine $m_{Punicine}$), a specific energy equivalent $E_{m,eq}$ is obtained, which is used to assess the comminution results.

$$E_{m,eq} \sim \frac{P_{eq}}{m_{Li-Aluminate} + m_{Punicine}} \cdot t \quad (6)$$

For the co-comminution of lithium aluminate with the Punicines, they are weighed together with the grinding balls in the jars of the planetary ball mill and comminuted for 3 or 6 min. The starting materials have the particle size distributions shown in Figure 1. While the lithium aluminate has a median value of approximately 30 µm, C_0-Punicine and C_{17}-Punicine have a median value of about 230 µm, and C_{10}-Punicine is slightly smaller, at 160 µm.

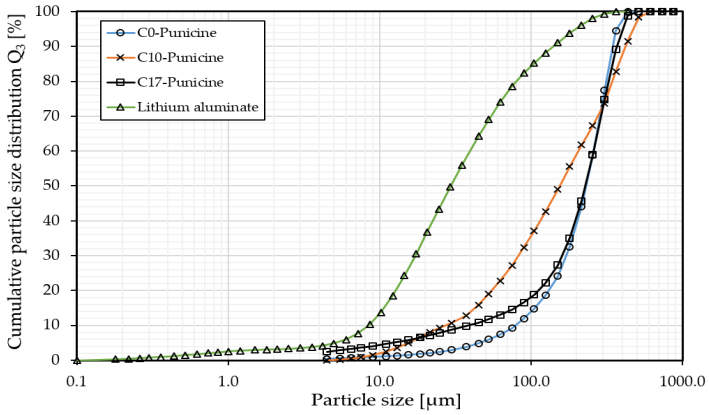

Figure 1. Particle size distributions of lithium aluminate and the different Punicines before the grinding process.

For the experiments, the types of Punicines and their concentrations were varied. Concentrations of 0.5%, 1%, and 5% were chosen. Punicine types vary in carbon chain lengths from 0 to 10 to 17 carbon atoms. This makes the Punicine molecule increasingly hydrophobic. The results for 0.5% and 1% are shown in Figure 2 and Figure 4, where either the volume-weighted mean particle size or the specific surface area is plotted against the equivalent specific energy $E_{m,eq}$. With 5%, which is multiple times the amount of additive required for flotation, only individual experiments were conducted.

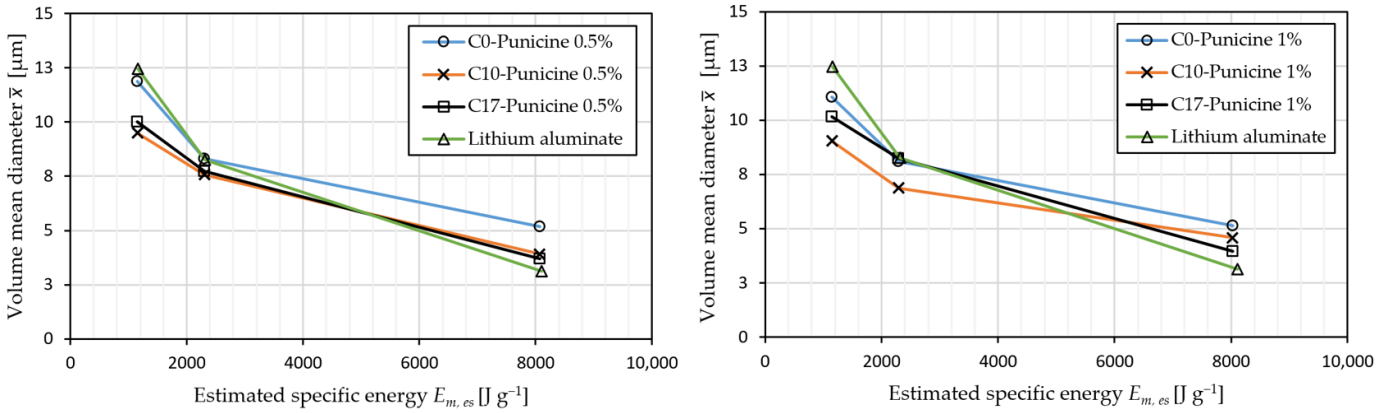

Figure 2. Mean particle size as a function of the equivalent specific energy for grinding lithium aluminate in pure form and with Punicines of different types and concentrations.

The particle size was measured in an aqueous environment, meaning that upon transfer of the ground particles, the Punicines can partially dissolve, and existing agglomerates can be dispersed through ultrasound treatment. For the comminution, it can be observed that without the addition of Punicines, a slightly less efficient comminution is initially observed compared to Punicine addition. For higher energy inputs, Punicines with decreasing chain lengths seem to inhibit the comminution kinetics compared to comminution without additives. Particularly noteworthy is C_{10}-Punicine at 1%, which appears to ensure significantly faster comminution for low energy inputs. For instance, after approximately 1000 J/g, mean particle sizes of 9 µm were achieved, while the pure material for the same energy input was still at 13 µm. Thus, Punicines seem to act as a grinding aid at the beginning.

Figure 3 shows the grinding result for 1100 kJ/kg with an increasing amount of C_{17}-Punicine dosed to the lithium aluminate. For the low concentration, nearly no influence on the amount of Punicine can be detected, only a slightly coarser particle size for the particle

size range above 10 µm is seen. If the Punicine amount is increased further, the whole distribution shifts to the right, meaning more ineffective grinding with 5% of C_{17}-Punicine.

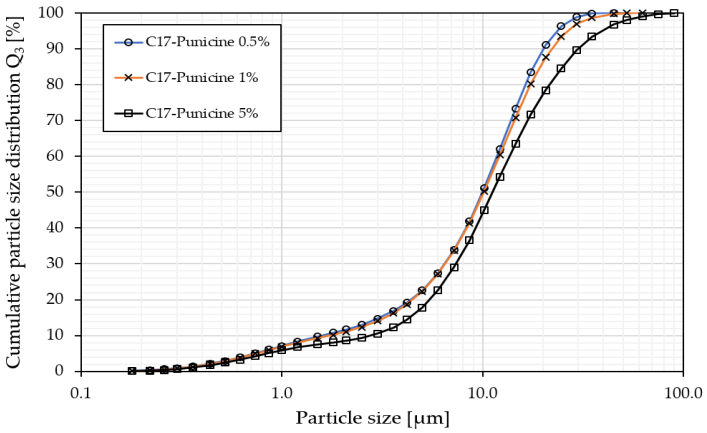

Figure 3. Particle size distribution for eq. spec. energy of 1100 kJ/kg in relation to the added amount of C_{17}-Punicine.

Figure 4 shows the specific surface areas over the equivalent specific energy. These were measured on dry powders and, for 0.5% Punicines, essentially no or nonsignificant influence of Punicine type on the increase in specific surface area was observed. For the 1% values, C_{10}-Punicine stands out as a more efficient comminution compared to the other Punicines. The natural product Punicine ("C_0-Punicine") seems to inhibit comminution as well as the more hydrophobic C_{17}-Punicine.

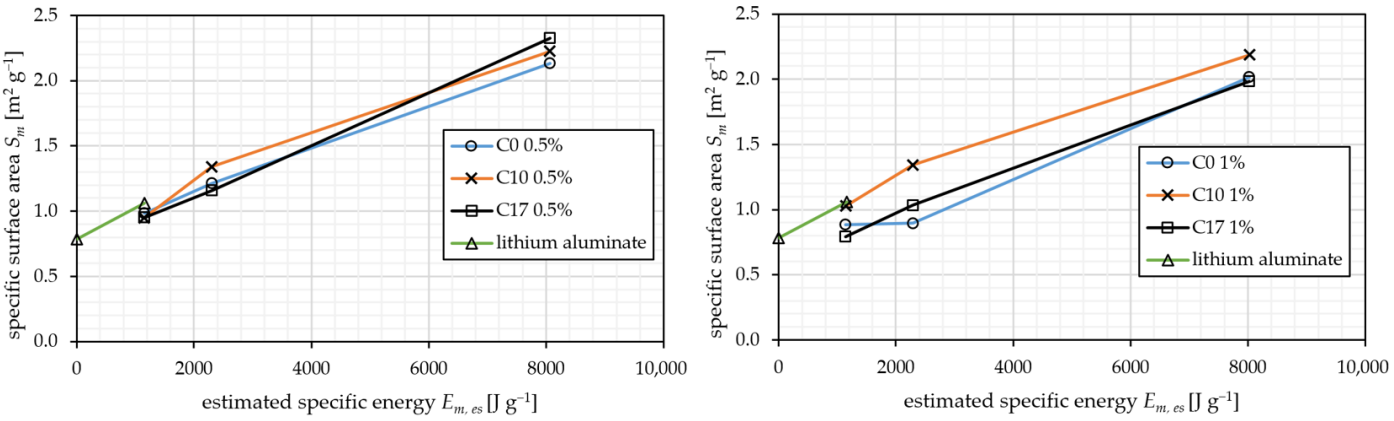

Figure 4. Specific surface vs. equivalent specific energy for lithium aluminate in pure form and with Punicines of different types and concentrations.

Punicines are soft solid organic particles with relatively coarse particle sizes at the beginning of the grinding process in comparison to lithium aluminate. Its breaking and deformation behavior is expected to be more plastic than brittle. With up to 5 wt.% of maximum material, the Puncine particle number is low when starting the experiment. Thus, it is expected that the Punicines are ground rather quickly at the beginning, without influencing the bulk behavior of the lithium aluminate much. With the decreasing particle size of the Punicines, the interactions with the surfaces of the lithium aluminate will increase. Moreover, temperature peaks of more than 100 °C can occur during dry grinding. At low concentrations, the Punicine additives cover the surfaces of lithium aluminate particles plastically forming thin layers. This results in reduced particle–particle interactions and thus reduced particle agglomeration, improving the comminution result. In contrast, excessive amounts of the Punicine additive, as in the 5% samples, could form thick layers on the particles dampening the impact stress and thus reducing the energy transferred onto

the lithium aluminate particles themselves, which would explain the negative impact on particle size reduction seen in Figure 3. The number of caught particles during one stress event will increase with increasing adhesion behavior, thus the stress intensity decreases, leading to a more inefficient grinding kinetic, because the agglomerates consume energy for their dispersion and less energy is divided to a higher number of particles during each stress event. Besides the physical behavior of the organic material, its molecular structure will influence the interaction with the aluminate surface and the agglomeration tendency [68].

For dry comminution in batch mills, Prizwara et al. showed that, in principle, an improvement in dry comminution of the mineral limestone can be achieved with organic additives, and their effect is related to the molecular structure or the proportions of polar and non-polar functional groups [69]. For instance, for alcohols, improved comminution was observed with increasing carbon chain length up to decanol, while for acids, very efficient comminution was observed with heptanoic acid, which decreased again with undecanoic acid. The mechanism of how these additives interact with the particle surface is still unclear, although the effect due to flowability could be shown. Here, it may be assumed that, especially, the C_{10}-Punicine has good proportions of hydrophobic to hydrophilic properties to keep grinding as efficiently as without additive.

3.2. Froth Flotation of Punicine-Functionalized Minerals

First, flotation experiments were performed on pure $LiAlO_2$ samples that were subject to different grinding parameters (Table 1). These serve as references to evaluate the effect of the functionalizing additives. No significant differences between the blank flotations are observed. These blank tests are consistent with the results of earlier experiments [45,50]. They can be attributed to the particle size in connection with a certain hydrophobicity of the surfaces.

Table 1. Flotation yields of blank tests. Flotation conditions were as follows: 1.00 g $LiAlO_2$, 32 cm^3/min air flow, 500 rpm stirring speed, 3 min, pH 11, brackets: 95% confidence intervals.

	Flotation Yield [%] with 95% Confidence Interval		
	$E_{m,eq}$ **= 1100 J g^{-1}**	$E_{m,eq}$ **= 8000 J g^{-1}**	$E_{m,eq}$ **= 2000 J g^{-1}**
Daylight	25.22 (8.39)	27.13 (2.70)	24.01 (9.76)
UV-C	19.98 (6.47)	25.98 (11.63)	23.44 (10.65)

Next, we investigated the flotation of minerals functionalized with Punicine, C_{10}-Punicine and C_{17}-Punicine, respectively (Figure 5). $LiAlO_2$ was milled with the addition of 0.5% and 1% of the aforementioned Punicines, respectively, at otherwise constant comminution parameters. As expected, C_0-Punicine without a hydrophobizing side chain had only a minor influence on the floatability of the mineral particles, as the flotation yields only increased from 25.22% (±8.39%) to around 30%, regardless of the amount of Punicine added. Under the influence of C_{10}- and C_{17}-Punicines, however, the flotation yield was significantly increased (Figure 5). Grinding with C_{10}-Punicine more than doubled the yields to 59.04% (±4.79%) and C_{17}-Punicine even gave nearly quantitative flotation results, which corresponds to an increase of about 70% compared to the blank samples. As expected, a larger hydrophobic moiety in the Punicine additive leads to a stronger hydrophobization of the mineral particle. As mentioned in the introduction, studies by Schmidt et al. have shown that the recovery rates of $LiAlO_2$ are light-dependent when Punicine derivatives are used as collectors in solution during the flotation experiment. This is due to altered nucleophilicity and thus altered mineral-collector interaction upon excitation to the radical state. As can be seen from Figure 5, light has less influence in the experiments described here, at least as far as 0.5% C_{17}-Punicine is concerned. However, there were clear differences for C_{10}-Punicine, depending on whether the flotation was carried out in daylight or under the influence of UV light. For example, the recovery rate increases by 36% (i.e., from 40.18%

to 54.70%) when 1% C_{10}-Punicine was added if the flotation was carried out in daylight instead of UV light. This is consistent with the formation of radical species, as shown in Scheme 1, under the influence of UV light. This is because these are radical cations and radical anions, i.e., charged, more hydrophilic species on the particle surfaces than the Punicines in the ground state. The influence of light on Punicines, which are only added as collectors during flotation, is different, as the adsorption process on the surface must first take place under these conditions.

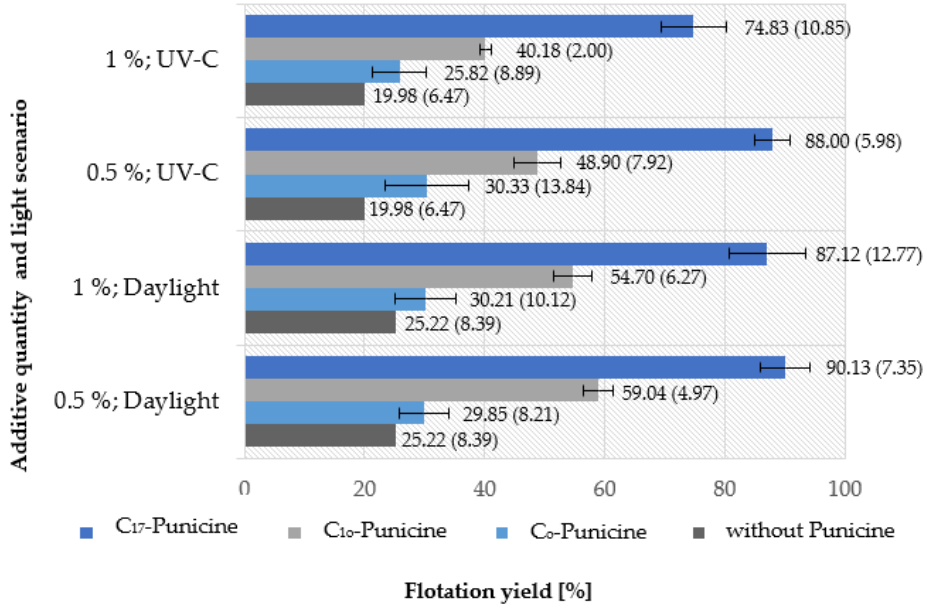

Figure 5. Flotation yields of functionalized $LiAlO_2$ (ground at $E_{m,eq}$ = 1100 J g^{-1}). Flotation conditions were as follows: 1.00 g $LiAlO_2$, 30 µL frother, 32 cm^3/min air flow, 500 rpm stirring speed, 3 min, pH 11. The 95% confidence intervals are in brackets.

Increasing the amount of Punicine from 0.5% to 1% does not seem to have a positive effect on the yield, as the flotation yield decreased by 8% for C_{10}-Punicine and by 3% for C_{17}-Punicine. To gain further insight, we also conducted flotation experiments with minerals loaded with 5% of C_{10}- and C_{17}-Punicines during comminution. These experiments confirmed that higher loadings than 0.5% of the additives do not improve the flotability of the minerals.

Changing the grinding parameters led to smaller particle sizes, as discussed in Section 3.1. This effect is also visible in the flotation results. Regardless of the additive, mineral samples that were comminuted with higher specific energy equivalents show lower yields in the microflotation experiments, e.g., under daylight conditions with C_{10}-Punicine (Figure 6). Since particle sizes around 20–100 µm show optimal results in flotation [69,70], the smaller particle sizes are the reason for the decrease in flotation efficiency. In order to exclude partial degradation of the Punicines during the grinding process, which would probably also lead to lower flotation yields, stability tests were carried out. For this purpose, we loaded the planetary ball mill with 4 g of pure C_{17}-Punicine and milled it for 10 min at 600 rpm. We then performed NMR and IR spectroscopic as well as mass spectrometric analyses of the organic components and were able to confirm that C_{17}-Punicine did not decompose even under these very rigorous conditions (c.f. Supplementary Materials for spectra). In summary, Punicines are stable compounds that can withstand even rigorous processing conditions without decomposing and retain their properties. While the higher concentrations of especially 1% of C_{10}-Punicine lead to increased photosensitivity of the flotation, the addition of only 0.5% C_{17}-Punicine prior to dry grinding in a planetary ball mill results in excellent recovery of lithium aluminate during flotation.

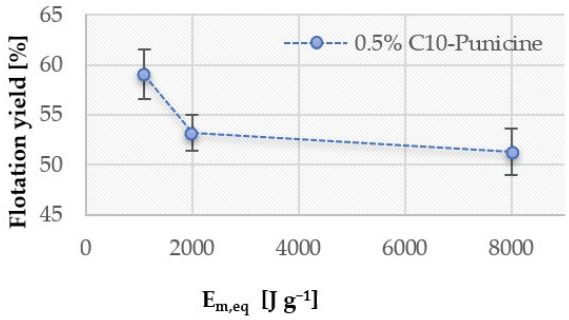

Figure 6. Flotation yields in dependence of comminution estimated specific energy. 1.00 g functionalized $LiAlO_2$, 30 µL frother, 32 cm^3/min air flow, 500 rpm stirring speed, 3 min, pH 11 and daylight.

3.3. Investigations of the Mechanism of In Situ Hydrophobization: Variation of the Addition Methods, IR-Spectroscopy, SEM Imaging and ICP–OES Measurements

To gain insight into the nature of the interaction between lithium aluminate and the Punicines that leads to the hydrophobization during the dry grinding, we investigated the effect of two other methods of Punicine addition to the mineral on flotation results. In addition to Punicine addition before the grinding process in the planetary ball mill described above (A), the effect of adding a solution of C_{17}-Punicine into the HALLIMOND tube (B) on the flotation results was investigated. Furthermore, C_{17}-Punicine was added to a planetary ball mill together with the lithium aluminate and mixed without grinding media for 3 min at 250 rpm (C). The yields of the respective microflotation experiments, including the blank sample without the addition of Punicine, are shown in Figure 7.

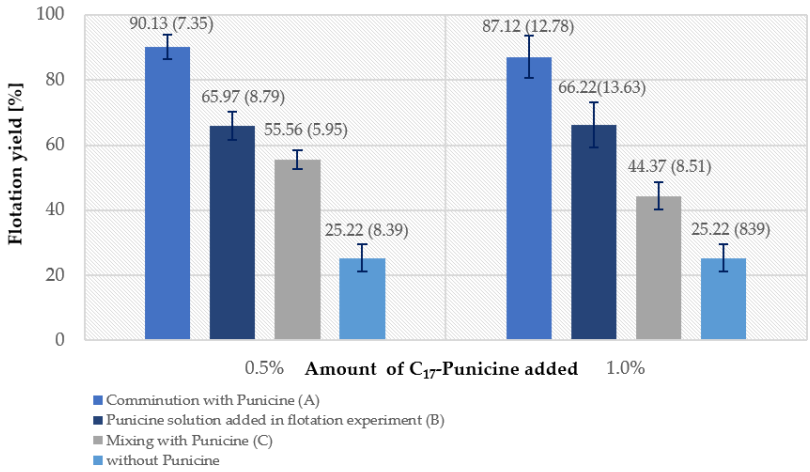

Figure 7. Flotation yields of $LiAlO_2$ under varying methods of C_{17}-Punicine addition. Flotation conditions were as follows: 1.00 g $LiAlO_2$, 30 µL frother, 32 cm^3/min air flow, 500 rpm stirring speed, 3 min. of flotation time, pH 11, daylight.

Figure 7 clearly shows that the dry grinding of lithium aluminate in the presence of C_{17}-Punicine gives the best recovery yields. The addition of Punicine solutions to ground lithium aluminate in the HALLIMOND tube gave significantly lower yields, while the subsequent mixing of both gave the poorest recovery rates. While we were able to prove in previous work that Punicine in an aqueous solution can react with the lithium aluminate hydroxide hydrate, which is undesirable for flotation, further parameters must be considered for the dry process to explain the hydrophobization. One possible explanation is the above-mentioned reaction of the Punicine in competition with water with the fresh surfaces of the lithium aluminate, whereby the nucleophilicity indices mentioned in the introduction support this hypothesis. In fact, the new surfaces are considered reactive towards their environment [17]. On the other hand, the creation of new surfaces through fractures can generate local temperature peaks ranging from several hundred to a thousand degrees

Celsius [71–73]. The originally particulate Punicines are not only ground and broken by the mechanical energy applied, but also plastically deformed and possibly even melted. Their melting temperatures are between 110 °C and 230 °C, i.e., temperatures that can be reached locally, especially under higher mechanical stress. It can be assumed that they are deposited on fresh surfaces [74,75] so that the hydrophobization can be attributed to chemisorption and physisorption. C_{17}-Punicine has the longest hydrophobic chain and can therefore protect the lithium aluminate surface most effectively from the surrounding moisture and suppress the formation of lithium aluminum hydroxide hydrate and carbonate hydrate of the three Punicine derivatives investigated. In fact, IR spectroscopic investigations of the $LiAlO_2$ sample milled in situ with Punicines showed a mere superposition of the individual IR spectra without band shifts or new absorption bands. They prove the coating of the $LiAlO_2$ particles with the undecomposed Punicines, as the characteristic absorptions of C_{17}-Punicine are visible as prominent bands at 2914.1 ($\nu_{alkyl\ chain}$), 1641.4, 1509.0, 1470.9 and 1546.4 cm^{-1}, among others. It is striking that the characteristic band at 529.7 cm^{-1}, which is due to the $\nu_4(\delta O\text{-}Al)$ vibration of $LiAl_2(OH)_6^+$ [76], is missing. The bands at 674.0, 725.5, 1352.1 and 1368.5 cm^{-1}, which are typical for water-treated lithium aluminate and thus lithium aluminate hydroxide hydrates [50], are also missing (c.f. Supplementary Materials). The hydrophobization by C_{17}-Punicine apparently protects the lithium aluminate particles from attack by water and from the formation of hydrophilic surfaces of $LiAl_2(OH)_7 \blacksquare xH_2O$ and other compounds derived thereof such as carbonates that are undesirable for flotation.

To gather further evidence, we took SEM images and analyzed the flotates using ICP–OES. Figure 8 shows SEM images of the milled products with increasing C_{17}-Punicine content from left to right (left: 0%, middle: 0.5%, right: 5%). The SEM images show a clear change in the resulting structures. When grinding without the addition of C_{17}-Punicine, an agglomerated structure is formed, partly with the characteristic platelet structures of lithium aluminum hydroxide hydrate or carbonate hydrate, as described by Beckermann et al. [48]. The particles are compact and angular in shape, with particle sizes ranging from a few micrometers to several tenths of a micrometer. Many fine structures can be seen on the coarser particles, some of which are platelet-shaped. The addition of Punicine reduces the fine structures on the coarser particles and the surfaces appear smoother. The structures remain aggregated but lose their platelet structure. The reason for this is the ambient moisture with which the lithium aluminate reacts. The formation of these platelet-like structures decreases with increasing C_{17}-Punicine content until they are finally barely recognizable in the image on the right. These visual impressions thus support the results of the IR-spectroscopic investigations.

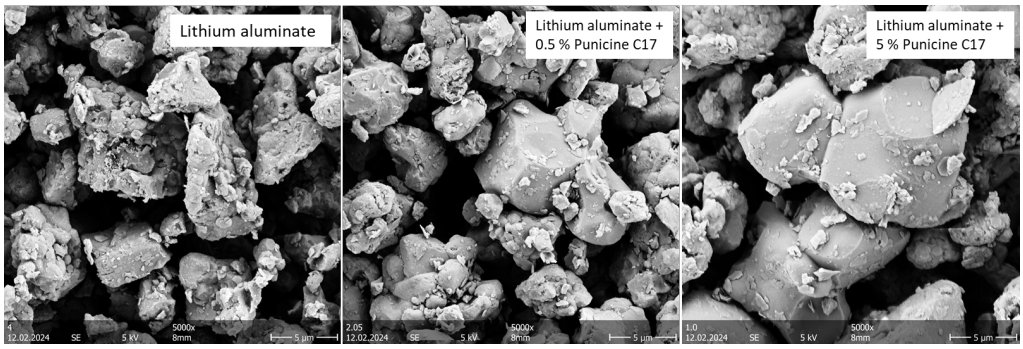

Figure 8. SEM images of the ground product for an equivalent specific energy input of 1150 J/g.

For flotation, this hydrophobization and the prevention of the formation of hydrophilic particle surfaces from hydroxides, carbonates and hydrates is not only a prerequisite, but it should also prevent the leaching of lithium ions mentioned in the introduction, which are lost for flotation. To verify this, we carried out ICP–OES measurements to determine the concentration of lithium ions in the filtrate of the flotation concentrate (Table 2). Untreated lithium aluminate, which was flotated for 3 min, served as a reference. Both samples were

subjected to the same comminution process prior to flotation. In line with the results of the SEM images and IR investigations, the lithium concentration in the flotation effluents was reduced by almost 40%. To further confirm this observation, we stirred 0.50 g of unfunctionalized $LiAlO_2$ in addition to $LiAlO_2$ ground with 5% C_{17}-Punicine in 100 mL of pure water and measured the pH change over time for each (Figure 9). Pure lithium aluminate reacts quickly with water according to Equations (1) and (2) (c.f. Section 1) so that a pH value of 10.5 is reached within 30 s. The mineral functionalized with C_{17}-Punicine-functionalized mineral, however, only reaches a pH of 10 after three minutes. It is clear that the hydrophobization of the mineral surface hinders the reaction with water to form basic $LiAl_2(OH)_x$ species as well as the leaching of lithium ions into the solution.

Table 2. Li and Al concentrations in the flotation filtrate after flotating untreated $LiAlO_2$ and $LiAlO_2$ ground with C_{17}-Punicine.

	Concentration Al in mg/L	Concentration Li in mg/L
$LiAlO_2$ pure	47.70	17.16
$LiAlO_2$ + 5% C_{17}-Punicine	16.82	10.40

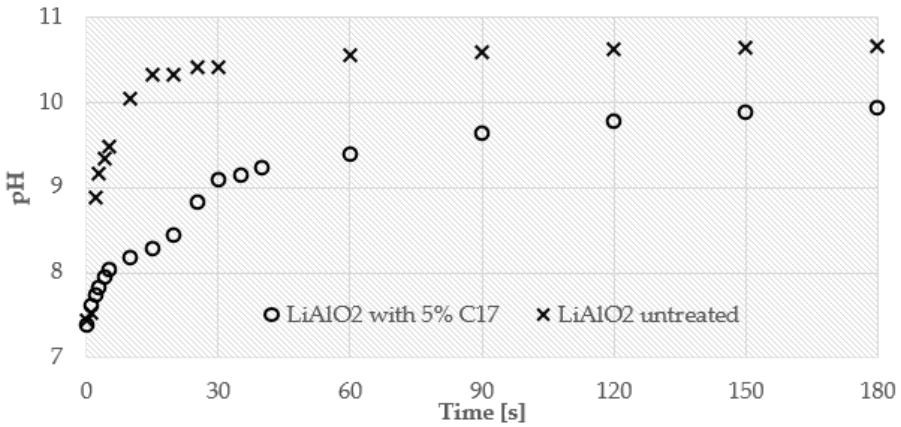

Figure 9. Change in pH as a function of time for lithium aluminate and Punicine-treated lithium aluminate in water.

4. Conclusions

Derivatives of the natural product Punicine from *Punica granatum* (pomegranates) are effective switchable collectors for the flotation of lithium aluminate and react with light and the pH of the medium. Adding two previously unreported derivatives to the product before the grinding process leads to well-ground particles, where the Punicines interact with the newly created surface and hydropobize the particles, depending on their structure. This hydrophobization of the particle surfaces during the grinding, which in turn leads to excellent recovery rates during flotation if the Punicines are provided with long hydrophobic alkyl chains such as C_{17}, is better than other methods for combining particles and Punicines. According to investigations using SEM microscopy, IR spectroscopy and pH measurements, Punicines protect the particles from attack by water in the method described here and thus from the formation of hydrophilic $LiAl_2(OH)_7 \blacksquare x\ H_2O$ layers that are undesirable for flotation. These cannot be detected after the dry grinding method described here and subsequent aqueous flotation. This also prevents the undesired bleeding of lithium cations from the lithium aluminate particles, which would be lost for lithium recycling by flotation of the engineered artificial mineral (EnAM) lithium aluminate. Higher concentrations of 1% lead to more pronounced photosensitivity of, for example, the C_{10}-Punicine on the particle surface of $LiAlO_2$. On the other hand, the addition of only 0.5% of C_{17}-Punicine before grinding leads to almost quantitative flotation results.

Supplementary Materials: The following supporting information can be downloaded at: https://www.mdpi.com/article/10.3390/min14070650/s1, Figures S1–S4: NMR spectra of Punicines; Figure S5: IR spectra of C17-Punicine; Figure S6: UV-Vis spectra of C0-Punicine; Figure S7: Hallimond Tube with dimensions; Figure S8: Specification of LEDs.

Author Contributions: Conceptualization, all authors; methodology, A.Z., M.H.F., F.S. and L.B.; validation, S.B.-F. and A.S.; formal analysis, A.S. and S.B.-F.; investigation and data curation, F.S., A.Z., M.H.F. and L.B.; writing—original draft preparation, A.S., M.H.F. and S.B.-F.; writing—review and editing, A.S. and S.B.-F.; visualization, L.B. and M.H.F.; supervision, A.S. and S.B.-F.; project administration, A.S. and S.B.-F.; funding acquisition, A.S. and S.B.-F. All authors have read and agreed to the published version of the manuscript.

Funding: This research was funded by the German Research Foundation (DFG) within the Priority Program 2315, grant number Br 4361/6-1 (project number 470377913) and Schm 1371/18-1 (project number 470324113).

Data Availability Statement: The original contributions presented in the study are included in the article and Supplementary Materials. Further inquiries can be directed to the corresponding authors.

Acknowledgments: We thankfully acknowledge Petra Lassen, IAAC TU Clausthal, for ICP–OES measurements. Furthermore, we thank Annett Wollmann and Peggy Knospe, IMVT TU Clausthal, for SEM imaging.

Conflicts of Interest: The authors declare no conflicts of interest.

References

1. European Critical Raw Materials Act. Available online: https://commission.europa.eu/strategy-and-policy/priorities-2019-2024/european-green-deal/green-deal-industrial-plan/european-critical-raw-materials-act_en (accessed on 18 March 2024).
2. Demand for Lithium Worldwide in 2020 and 2021 with a Forecast from 2022 to 2035. Available online: https://www.statista.com/statistics/452025/projected-total-demand-for-lithium-globally/ (accessed on 18 March 2024).
3. Yang, D.; Chen, G.; Zhang, L.; Chen, Z.; Zhang, R.; Asghar, M.I.; Geng, S.; Lund, P.D. Low temperature ceramic fuel cells employing lithium compounds: A review. *J. Power Sources* **2021**, *503*, 120070. [CrossRef]
4. Venkateswaran, C.; Sreemoolanadhan, H.; Vaish, R. Lithium aluminosilicate (LAS) glass-ceramics: A review of recent progress. *Int. Mater. Rev.* **2022**, *67*, 620–657. [CrossRef]
5. Bahel, S.; Singh, R.; Kaur, G.; Narang, S.B. Low fire M-phase lithium based dielectric ceramics for microwave applications: A review. *Ferroelectrics* **2016**, *502*, 49–56. [CrossRef]
6. Naumov, A.S.; Alkeseev, R.O.; Savinkov, V.I.; Sigaev, V.N. Nucleation and Crystals Growth in the Volume of Glass Li_2O-Al_2O_3-SiO_2 System. *Glass Ceram.* **2023**, *96*, 3–11. [CrossRef]
7. Huang, S.J.; Wang, W.Z.; Jiang, H.; Zhao, H.F.; Ma, Y.P. Network Structure and Properties of Lithium Aluminosilicate Glass. *Materials* **2022**, *15*, 4555. [CrossRef]
8. Yeh, F.M.; Volli, V.; Bin, L.W.; Tung, P.H.; Shu, C.M. Oxidative stability and thermal performance of ester based lube oil with lithium salt additives. *Appl. Therm. Eng.* **2019**, *150*, 1328–1336. [CrossRef]
9. Song, Z.H.; Liang, Y.M.; Fan, M.J.; Zhou, F.; Liu, W.M. Lithium-based ionic liquids functionalized by sym-triazine and cyclotriphosphazene as high temperature lubricants. *Tribol. Int.* **2014**, *70*, 136–141. [CrossRef]
10. Rivera, W.; Moreno-Quintanar, G.; Rivera, C.O.; Best, R.; Martinez, F. Evaluation of a solar intermittent refrigeration system for ice production operating with ammonia/lithium nitrate. *Sol. Energy* **2011**, *85*, 38–45. [CrossRef]
11. Sedighi, K.; Farhadi, M.; Liaghi, M. Exergy analysis: Parametric study on lithium bromide-water absorption refrigeration systems. *Proc. Inst. Mech. Eng. C J. Mech. Eng. Sci.* **2007**, *221*, 1345–1351. [CrossRef]
12. Stefanelli, E.; Puccini, M.; Pesetti, A.; Lo Frano, R.; Aquaro, D. Lithium orthosilicate as nuclear fusion breeder material: Optimization of the drip casting production technology. *Nuclear Mater. Energy* **2022**, *30*, 101131. [CrossRef]
13. Cao, Y.; Tan, S.L.; Cheung, E.J.H.; Siew, S.Y.; Li, C.J.; Liu, Y.; Tan, C.S.; Lal, M.; Chen, G.Y.; Dogheche, K.; et al. A Barium Titatnate-on-Oxide Insulator Optoelectronics Platform. *Adv. Mater.* **2021**, *33*, 2101128. [CrossRef]
14. Schirmer, T.; Qiu, H.; Li, H.; Goldmann, D.; Fischlschweiger, M. Li-Distribution in Compounds of the Li_2O-MgO-Al_2O_3-SiO_2-CaO System–A First Survey. *Metals* **2020**, *10*, 1633. [CrossRef]
15. Schirmer, T.; Qiu, H.; Goldmann, D.; Stallmeister, C.; Friedrich, B. Influence of P and Ti on Phase Formation at Solidification of Synthetic Slag Containing Li, Zr, La, and Ta. *Minerals* **2022**, *12*, 310. [CrossRef]
16. Wittkowski, A.; Schirmer, T.; Qiu, H.; Goldmann, D.; Fittschen, U.E.A. Speciation of Manganese in a Synthetic Recycling Slag Relevant for Lithium Recycling from Lithium-Ion Batteries. *Metals* **2021**, *11*, 188. [CrossRef]
17. Chelgani, S.C.; Parian, M.; Parapari, P.S.; Ghorbani, Y.; Rosenkranz, J. A Comparative Study on the Effects of Dry and Wet Grinding on Mineral Flotation Separation—A Review. *J. Mater. Res. Technol.* **2019**, *8*, 5004–5011. [CrossRef]

18. Li, J.; Hitch, M. Ultra-Fine Grinding and Mechanical Activation of Mine Waste Rock Using a Planetary Mill for Mineral Carbonation. *Int. J. Miner. Process.* **2017**, *158*, 18–26. [CrossRef]
19. Mohammadnejad, S.; Provis, J.L.; van Deventer, J.S.J. Effects of Grinding on the Preg-Robbing Potential of Quartz in an Acidic Chloride Medium. *Miner. Eng.* **2013**, *52*, 31–37. [CrossRef]
20. Liu, J.; Long, H.; Corin, K.C.; O'Connor, C.T. A Study of the Effect of Grinding Environment on the Flotation of Two Copper Sulphide Ores. *Miner. Eng.* **2018**, *122*, 339–345. [CrossRef]
21. Jung, H.J.; Sohn, Y.; Sung, H.G.; Hyun, H.S.; Shin, W.G. Physicochemical Properties of Ball Milled Boron Particles: Dry vs. Wet Ball Milling Process. *Powder Technol.* **2015**, *269*, 548–553. [CrossRef]
22. Bocharov, V.A.; Ignatkina, V.A. On Regularities Observed in Formation of Liquid Phase Composition in Flotation Sulfide Pulp. *J. Min. Sci.* **2007**, *43*, 98–108. [CrossRef]
23. Lin, H.K.; Walsh, D.E.; Yen, H. Effects of Tramp Grinding Steel and Iron Fines on Comminution, Flotation and Cyanidation. *Min. Metall. Explor.* **2013**, *30*, 191–196. [CrossRef]
24. Feng, D.; Aldrich, C. A Comparison of the Flotation of Ore from the Merensky Reef after Wet and Dry Grinding. *Int. J. Miner. Process.* **2000**, *60*, 115–129. [CrossRef]
25. Seke, M.D.; Pistorius, P.C. Effect of Cuprous Cyanide, Dry and Wet Milling on the Selective Flotation of Galena and Sphalerite. *Miner. Eng.* **2006**, *19*, 1–11. [CrossRef]
26. Palm, N.A.; Shackleton, N.J.; Malysiak, V.; O'Connor, C.T. The Effect of Using Different Comminution Procedures on the Flotation of Sphalerite. *Miner. Eng.* **2010**, *23*, 1053–1057. [CrossRef]
27. Koleini, S.M.J.; Abdollahy, M.; Soltani, F. Wet and dry Grinding Methods effect on the Flotation of Taknar Cu-Zn Sulfide ore using a mixed collector. In Proceedings of the 26th International Mineral Processing Congress, IMPC, New Delhi, India, 24–28 September 2012. [CrossRef]
28. Peltoniemi, M.; Kallio, R.; Tanhua, A.; Luukkanen, S.; Perämäki, P. Mineralogical and Surface Chemical Characterization of Flotation Feed and Products after Wet and Dry Grinding. *Miner. Eng.* **2020**, *156*, 106500. [CrossRef]
29. Zhu, G.; Wang, Y.; Liu, X.; Yu, F.; Lu, D. The Cleavage and Surface Properties of Wet and Dry Ground Spodumene and Their Flotation Behavior. *Appl. Surf. Sci.* **2015**, *357*, 333–339. [CrossRef]
30. Xu, L.; Hu, Y.; Wu, H.; Tian, J.; Liu, J.; Gao, Z.; Wang, L. Surface Crystal Chemistry of Spodumene with Different Size Fractions and Implications for Flotation. *Sep. Purif. Technol.* **2016**, *169*, 33–42. [CrossRef]
31. Zhu, G.; Wang, Y.; Wang, X.; Miller, J.D.; Lu, D.; Zheng, X.; Zhao, Y.; Zheng, H. Effects of Grinding Environment and Lattice Impurities on Spodumene Flotation. *Trans. Nonferrous Met. Soc. China* **2019**, *29*, 1527–1537. [CrossRef]
32. Tanhua, A.; Peltoniemi, M.; Kallio, R.; Peräniemi, S.; Luukkanen, S. The Effects of Dry Grinding and Chemical Conditioning during Grinding on the Flotation Response of a Cu-Zn Sulphide Ore and a Spodumene Pegmatite Silicate Ore. *Miner. Eng.* **2022**, *189*, 107865. [CrossRef]
33. Wills, B.A.; Napier-Munn, T. *Mineral Processing Technology: An Introduction to the Practical Aspects of Ore Treatment and Mineral Recovery*; Elsevier: Amsterdam, The Netherlands, 2006; p. 267, ISBN 0750644508.
34. Nguyen, A.V.; Schulze, H.J. *Colloidal Science of Flotation*; Marcel Dekker: New York, NY, USA, 2004; ISBN 0824747828.
35. Weng, X.; Mei, G.; Zhao, T. Utilization of novel ester-containing quaternary ammonium surfactant as cationic collector for iron ore flotation. *Sep. Purif. Technol.* **2013**, *103*, 187–194. [CrossRef]
36. Lima, R.N.G.; Brandao, P.R.G.; Peres, A.E.C. The infrared spectra of amine collectors used in the flotation of iron ores. *Miner. Eng.* **2005**, *18*, 267–273. [CrossRef]
37. Xing, Y.; Xu, M.; Gui, X.; Cao, Y.; Babel, B.; Rudolph, M.; Weber, S.; Kappl, M.; Butt, H.-J. The application of atomic force microscopy in mineral flotation. *Adv. Colloid Interface Sci.* **2018**, *256*, 373–392. [CrossRef]
38. Hunter, T.N.; Pugh, R.J.; Franks, G.V.; Jameson, G.J. The role of particles in stabilizing foams and emulsions. *Adv. Colloid Interface Sci.* **2008**, *137*, 57–81. [CrossRef] [PubMed]
39. Polat, H.; Erdogan, D.J. Heavy metal removal from waste waters by ion flotation. *Hazardous Mater.* **2007**, *148*, 267–273. [CrossRef]
40. Rahman, R.M.; Ata, S.; Jameson, G.J. The effect of flotation variables on the recovery of different particle size fractions in the froth and the pulp. *Int. J. Miner. Process.* **2012**, *106*, 70–77. [CrossRef]
41. Zamboulis, D.; Pataroudi, S.; Zouboulis, A.; Matis, K. The application of sorptive flotation for the removal of metal ions. *Desalination* **2004**, *162*, 159–168. [CrossRef]
42. Filippov, L.; Farrokhpay, S.; Lyo, L.; Filippova, I. Spodumen Flotation Mechanism. *Minerals* **2019**, *9*, 372. [CrossRef]
43. Tian, J.; Xu, L.; Wu, H.; Fang, S.; Deng, W.; Peng, T.; Sun, W.; Hu, Y. A novel approach for flotation recovery of spodumene, mica and feldspar from a lithium pegmatite ore. *J. Clean. Prod.* **2018**, *174*, 625–633. [CrossRef]
44. Lithium Aluminate. Available online: https://www.chemicalbook.com (accessed on 18 March 2024).
45. Zgheib, A.; Fischer, M.H.; Namyslo, J.C.; Fittschen, U.E.A.; Wollmann, A.; Weber, A.P.; Schmidt, A. Photo-switchable Collectors for the Flotation of Lithium Aluminate for the Recycling of the Critical Raw Material Lithium. *ChemSusChem* **2024**, *in print*. [CrossRef]
46. Thiel, J.P.; Chiang, C.K.; Poeppelmeier, K.R. Structure of lithium aluminum hydroxide dihydrate ($LiAl_2(OH)_7 \cdot 2H_2O$). *Chem. Mater.* **1993**, *5*, 297–304. [CrossRef]
47. Kropachev, A.; Kalabskiy, I. Hydrometallurgical preparation of lithium aluminum carbonate hydroxide hydrate $Li_2Al_4(CO_3)(OH)_{12} \cdot 3H_2O$ from aluminate solution. *Miner. Eng.* **2020**, *155*, 106470. [CrossRef]

48. Beckermann, S.J.; Ford, R.B.; Nemeth, M.T. Conversion of gamma lithium aluminate to lithium aluminum carbonate hydroxide hydrate. *Powder Diffr.* **1996**, *11*, 312–317. [CrossRef]
49. Nemeth, M.T.; Ford, R.B.; Taylor, T.A. Analysis of Mixtures of Gamma Lithium Aluminate, Lithium Aluminum Carbonate Hydroxide Hydrate, and Lithium Carbonate. *MRS Online Proc. Libr.* **1997**, *496*, 159–165. [CrossRef]
50. Zgheib, A.; Acker, S.; Fischer, M.H.; Namyslo, J.C.; Strube, F.; Rudolph, M.; Fittschen, U.E.A.; Wollmann, A.; Weber, A.P.; Nieger, M.; et al. Lithium aluminate flotation by pH- and light-switchable collectors based on the natural product Punicine. *RSC Adv.* **2024**, *14*, 9353–9364. [CrossRef] [PubMed]
51. Nawwar, M.A.; Hussein, S.A.; Merfort, I. Leaf phenolics of Punica granatum. *Phytochemistry* **1994**, *37*, 1175. [CrossRef]
52. Schmidt, A.; Mordhorst, T.; Nieger, M. Investigation of a betainic alkaloid from Punica granatum. *Nat. Prod. Res.* **2005**, *19*, 541–546. [CrossRef] [PubMed]
53. Schmidt, A.; Mordhorst, T. Conjugated, cross-conjugated, and pseudo-cross-conjugated derivatives of a pyridinium alkaloid from Punica granatum. *Arkivoc* **2003**, *14*, 233–245. [CrossRef]
54. Otto, C.F.; Liu, M.; Herzberger, C.; Namyslo, J.C.; Nieger, M.; Hübner, E.G.; Lederle, F.; Freese, T.; Schmidt, A. Borane adducts of Punicine and of its dehydroxy derivatives (pyridinium-1-yl)-2- and 3-phenolates. *Tetrahedron* **2020**, *76*, 131627. [CrossRef]
55. Nagorny, S.; Lederle, F.; Udachin, V.; Weingartz, T.; Hübner, E.G.; Dahle, S.; Maus-Friedrichs, W.; Adams, J.; Schmidt, A. Switchable Mesomeric Betaines Derived from Pyridinium-Phenolates and Bis(thienyl)ethane. *Eur. J. Org. Chem.* **2021**, *2021*, 3178–3189. [CrossRef]
56. Albrecht, M.; Yulikov, M.; Kohn, T.; Jeschke, G.; Adams, J.; Schmidt, A. Pyridinium salts and ylides as partial structures of photoresponsive Merrifield resins. *J. Mater. Chem.* **2010**, *20*, 3025–3034. [CrossRef]
57. Schmidt, A.; Albrecht, M.; Mordhorst, T.; Topp, M.; Jeschke, G. Studies on photocatalytically active materials containing structure elements of a pyridinium alkaoid from Punica granatum. *J. Mater. Chem.* **2007**, *17*, 2793–2800. [CrossRef]
58. Schmidt, A.; Mordhorst, T.; Fleischhauer, H.; Jeschke, G. Coupled photocatalytic electron-transfers with 4,4′- bipyridinium derivatives of a betaine alkaloid from Punica granatum. *Arkivoc* **2005**, *10*, 150–164. [CrossRef]
59. Albrecht, M.; Gjikaj, M.; Schmidt, A. Intermolecular interactions of punicin derivatives. *Tetrahedron* **2010**, *66*, 7149–7154. [CrossRef]
60. Enguita, F.J.; Leitã, A.L. Hydroquinone: Environmental Pollution, Toxicity, and Microbial Answers. *BioMed Res. Int.* **2013**, *2013*, 542168. [CrossRef] [PubMed]
61. Deisinger, P.J.; Hill, T.S.; English, J.C. Human exposure to naturally occurring hydroquinone. *J. Toxicol. Environ. Health* **1996**, *47*, 31–46. [CrossRef] [PubMed]
62. Sims, G.K.; O'Loughlin, E.J.; Crawford, R.L. Degradation of pyridines in the environment. *Crit. Rev. Environ. Control.* **1989**, *19*, 309–340. [CrossRef]
63. Minegishi, S.; Kobayashi, S.; Mayr, H. Solvent Nucleophilicity. *J. Am. Chem. Soc.* **2004**, *126*, 5174–5181. [CrossRef] [PubMed]
64. Mayer, R.J.; Breugst, M.; Hampel, N.; Ofial, A.R.; Mayr, H. Ambident Reactivity of Phenolate Anions Revisited: A Quantitative Approach to Phenolate Reactivities. *J. Org. Chem.* **2019**, *84*, 8837–8858. [CrossRef] [PubMed]
65. Kwade, A. A Stressing Model for the Description and Optimization of Grinding Processes. *Chem. Eng. Technol.* **2003**, *26*, 199–205. [CrossRef]
66. Kwade, A. Mill Selection and Process Optimization Using a Physical Grinding Model. *Int. J. Miner. Process.* **2004**, *74*, S93–S101. [CrossRef]
67. Burmeister, C.; Titscher, L.; Breitung-Faes, S.; Kwade, A. Dry Grinding in Planetary Ball Mills: Evaluation of a Stressing Model. *Adv. Powder Technol.* **2018**, *29*, 191–201. [CrossRef]
68. Miethke, L.; Prziwara, P.; Finke, J.H.; Breitung-Faes, S. Opposing Effects of Additives in Dry Milling and Tableting of Organic Particles. *Pharmaceutics* **2021**, *9*, 1434. [CrossRef]
69. Prziwara, P.; Breitung-Faes, S.; Kwade, A. Impact of Grinding Aids on Dry Grinding Performance, Bulk Properties and Surface Energy. *Adv. Powder Technol.* **2018**, *29*, 416–425. [CrossRef]
70. Norori-McCormac, A.; Brito-Parada, P.R.; Hadler, K.; Cole, K.; Cilliers, J.J. The effect of particle size distribution on froth stability in flotation. *Sep. Purif. Technol.* **2017**, *184*, 240–247. [CrossRef]
71. Weichert, R.; Schönert, K. Heat Generation at the Tip of a Moving Crack. *J. Mech. Phys. Solids* **1978**, *26*, 151–161. [CrossRef]
72. Guduru, P.R.; Zehnder, A.T.; Rosakis, A.J.; Ravichandran, G. Dynamic Full Field Measurements of Crack Tip Temperatures. *Eng. Fract. Mech.* **2001**, *68*, 1535–1556. [CrossRef]
73. Pandey, K.N.; Chand, S. Analysis of Temperature Distribution near the Crack Tip under Constant Amplitude Loading. *Fatigue Fract. Eng. Mater. Struct.* **2008**, *31*, 316–326. [CrossRef]
74. Sonoda, R.; Horibe, M.; Oshima, T.; Iwasaki, T.; Watano, S. Improvement of Dissolution Property of Poorly Water-Soluble Drug by Novel Dry Coating Method Using Planetary Ball Mill. *Chem. Pharm. Bull.* **2008**, *56*, 1243–1247. [CrossRef] [PubMed]
75. Zhang, Q.; Wang, P.; Teng, S.; Qian, Z.; Zhu, L.; Gogos, C.G. Simultaneous Milling and Coating of Inorganic Particulates with Polymeric Coating Materials Using a Fluid Energy Mill. *Polym. Eng. Sci.* **2010**, *50*, 2366–2374. [CrossRef]
76. Dutta, P.K.; Puri, M. Anion Exchange in Lithium Aluminate Hydroxides. *J. Phys. Chem.* **1989**, *93*, 376–381. [CrossRef]